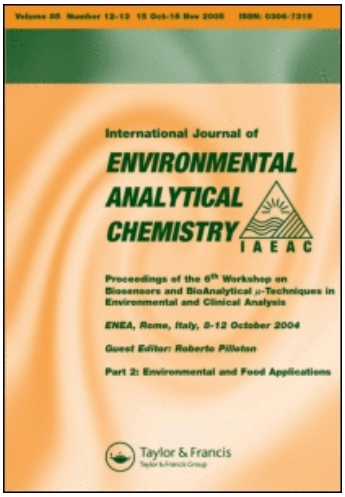

International Journal of Environmental Analytical Chemistry
Publication details, including instructions for authors and subscription information:
http://www.informaworld.com/smpp/title~content=t713640455

Biocompatible interfaces for biosensors

Andrew Gill[a]; Geoffrey Lillie[a]; Giosi Farace[b]; Pankaj Vadgama[b]
[a] Department of Clinical Biochemistry, Hope Hospital, University of Manchester, Manchester, UK [b] IRC in Biomedical Materials, Queen Mary, University of London, London E1 4NS, UK

To cite this Article Gill, Andrew , Lillie, Geoffrey , Farace, Giosi and Vadgama, Pankaj(2005) 'Biocompatible interfaces for biosensors', International Journal of Environmental Analytical Chemistry, 85: 9, 699 — 725
To link to this Article: DOI: 10.1080/03067310500155129
URL: http://dx.doi.org/10.1080/03067310500155129

Intern. J. Environ. Anal. Chem.
Vol. 85, Nos. 9–11, 10 August–15 September 2005, 699–725

Taylor & Francis
Taylor & Francis Group

Biocompatible interfaces for biosensors

ANDREW GILL†, GEOFFREY LILLIE†, GIOSI FARACE‡
and PANKAJ VADGAMA*‡

†Department of Clinical Biochemistry, Hope Hospital, University of Manchester, Manchester, UK
‡IRC in Biomedical Materials, Queen Mary, University of London, Mile End Road, London E1 4NS, UK

(*Received 14 September 2004; in final form 7 December 2004*)

Electrochemical biosensors need to interface reliably with complex biological samples. The latter are characterized by high surface activity and the presence of numerous interferent molecules. Polymeric membranes through their ability to act as surface modifiers of biosensors and as selective barriers help to minimize selectivity and biocompatibility problems for biosensors. Membranes studied include those based on PVC, polyether sulphone and cellulose acetate variously incorporating surfactants and as unmodified films to create a spectrum of permeabilities and surface properties. Additionally, electropolymerized phenolics as thin films have been tested as surface modifiers for base Pt working electrodes. Polypyrrole loaded with protein affinity molecules can register impedimetric change following target molecule binding – the avidin–biotin model system was used to exemplify this. Ultimately, fluid flow over a device can create a fully biocompatible, selective interface and operational viability was tested in preliminary studies using microfluid flow channels.

Keywords: PVC; Cellulose acetate; Polyphenol; Polypyrrole; Microfluidic; Biosensor; Electrochemical; Biocompatibility

1. Introduction

1.1 *Biosensor utility*

Biosensors provide a high degree of elegance in regard to their simple juxtaposition of bioreagent and transducer function. There is a direct alignment, thereby, of a functionally responsive biolayer, and the transducer element is able to directly extract the binding information from the encounter with analyte. There is a difficulty associated with such a simple, structurally inflexible combination, in that optimization is limited, as compared with the use of liquid phase bioreagent with its attendant optimized solution parameters of pH, pI, concentration and reagent additives. However, the net result is a solid-state, monolithic structure with the potential to deskill

*Corresponding author. Fax: +44-20-89831799. Email: p.vadgama@qmul.ac.uk

International Journal of Environmental Analytical Chemistry
ISSN 0306-7319 print: ISSN 1029-0397 online © 2005 Taylor & Francis
DOI: 10.1080/03067310500155129

analysis and to operate, moreover, in an optically opaque sample. For biomedicine, the latter facility holds considerable advantages, since most if not all biofluids contain colloid material that is liable to render the sample optically opaque, or at the very least to induce light scatter with the effect of degrading measurement accuracy in the majority of clinical sample assays, which rely on absorbance techniques.

1.2 *Biosensor drawbacks*

The established biosensor systems operate on the 'macro' scale, and have seen varying degrees of clinical exploitation [1]. A key reason for a limited introduction into the application domain has been the rapid alteration of the biosensor interface through the surface activity of the colloidal elements of any unmodified biological sample.

1.3 *Blood interfacing*

The most significant of the colloidal components in blood are proteins (albumin, globulins, complement) and formed elements (red cells, neutrophils, platelets, other immunologically competent cells). The subject of materials biocompatibility [2, 3] is a well-established one in regard to the biomaterials field, but the difference with respect to biosensors is that the surface fouling that results has an impact within seconds or minutes rather than the slow, chronic process of functional loss seen for example in the case of haemodialysis membranes and vascular stents, where surface fouling effects are minimal unless they reach the stage of major clot formation.

1.4 *Tissue interfacing*

There is a further special consequence of tissue implantation of biosensors, in that the implanted sensor component serves as a focus for the body's rejection of a foreign surface, with a classical foreign body reaction cascade set up. This again is a topic that has received enormous attention over the years as a proper domain of biomedical materials, but in reality, the tissue response to an implant is no different to that of a biosensor, with the exception that the implant reaction has the ability to degrade functional biosensor activity within seconds and minutes, in contrast to the adverse impact upon say bone replacement materials, artificial articulating surfaces, ocular lenses, etc. The nature of the tissue response is one of exudation of protein rich fluid, migration/adhesion of inflammatory cells, growth and building up of vascular connective tissue and eventually, the walling off of the implant by a denser band of avascular, collagen rich connective tissue.

1.5 *Biosensors and bioresponse compromise*

Whilst the bulk amount of protein, colloid and cell transfer to a 'clear' biosensor surface may be relatively low in amount, its diffusional barrier effect on the continued flux of analyte to a responsive biolayer surface will immediately be registered as a reduced biosensor response. The function of any flux dependent biosensor, unless it is merely a qualitative registering device, will be affected sufficiently that accuracy and precision of measurement will be lost, and neither may be recovered simply by recalibration.

The devices therefore likely to be most affected will be those using degrading enzymes rather than where a true binding equilibrium is approached, e.g. antibody, lectins, receptors and DNA/RNA. In the case of the latter group, the only effect should be on the rate of approach to equilibrium not on its final value, unless of course the fouling biolayer affects solute partitioning. This is possible in principle if say the fouling layer is a charged colloid, and the analyte target is also charged; electrostatic forces are then liable to come into play to either partition in or partition out a given analyte. Exclusion, furthermore, is possible if the analyte target is a macromolecule, in which case it may have limited access to the affinity surface of the biosensor through the limited porosity of the colloid fouling layer.

The underlying transducer of the biosensor, whilst not directly affected by surface colloidal deposits may register the presence of these non-specific elements through its detection domain. Thus the evanescent wave of an optical wave-guide or SPR system will respond equally to non-specific binding as to specific affinity interactions.

Passivation of the transducer element is possible with some surface-active crystalloids. Thus free amino acids and thiol-containing molecules that are surface active can distort and depress the catalytic behaviour of a Pt working electrode used for redox dependent biosensors.

1.6 *Biosensors and the selectivity compromise*

Whilst the biological component of a biosensor has recognised selectivity properties, and is *de facto* the driver for biosensor development, the underlying transducer whether based on electrochemical, potentiometric, optical or microgravimetric principles is vulnerable to a false positive response due to the surface activity of analogue species of either the target molecule or a molecule that is part of the transduction cascade. The most potent expression of the problem is where an electrically polarised noble metal electrode is used to detect the H_2O_2 product of an oxidase enzyme catalysed reaction in an enzyme electrode. At the typical polarizing voltage of +0.65 V *versus* Ag/AgCl, numerous species in biological solution are simultaneously oxidased, and false positive responses therefore result [4].

1.7 *Interfacial problems at microfabricated biosensors*

The issues of direct biosample interfacing of biosensors applies to all biosensors irrespective of length scale. So whilst the x–y plane architecture may be geometrically precise and formulated in a much more reproductive manner using MEMs and other microforming technologies, the biological response of the host sample reacts in rather similar ways, with adverse build up along the z axis, i.e. normal to the sensor surface. One rider in this equivalence of macro/microsensor outcomes is where response is flux (continuous diffusion) dependent; a sufficiently small sensing microsurface will have spherical and not planar diffusion, based on supply of analyte and is thereby less affected by external variables such as fouling. There is also evidence that a microstructure may set up a lower intensity tissue reaction thus leading to reduced surface fouling.

2. Membranes for biosensor interfacing

2.1 *Polymer membrane types*

Polymer, rather than inorganic membranes have been used from the start of biosensor technology to separate a sample from the sensing components. As packaging and separation phases, they do undoubtedly offer some useful solutions to the interfacing of biosensors with complex sample matrices. This sub-area amounts to a materials sciences effort in the development of both low fouling and high selectivity barrier structures.

Membranes may be classified according to their polymeric constituents (charged, neutral, amphiphilic), and their structural anisotropy; the most convenient and relevant for biosensors is the classification based upon available pore size. On the larger scale, there are standard filters of 100 μm pore diameter; microfiltration membranes of 1–10 μm pore size are used to separate viruses and whole cells; ultrafiltration >10 nm membranes are used to discriminate macromolecules and colloids; reverse osmosis membranes nominally of lower pore size are able to resolve small organics and ions, though in reality these have no discrete pore architecture. All of these can be used as a variable route to aperture control on a biosensor, no less for a biochip than for a conventional biosensor.

2.2 *Membrane property requirement*

Important surface properties to consider (table 1) depend upon the biomatrix application. Whilst great emphasis was placed in the past on hydrophobicity and a negative charge, in order to nominally reduce the deposition of negatively charged cells and to avoid polar purchase sites for hydrophilic protein domain interactions, in practice, neither approach can be relied upon in most cases. The adverse surface interactions have proven rather more subtle. There is a strong possibility that membrane surface feature size and profile is important, and that an ideally 'perfect', smooth surface would encounter minimum biofouling. Also surface fluidity on the micron scale, analogous to cell membrane fluidity may be a means of avoiding protein cell adsorption. Phosphorylcholine (PC) has both positive and negative charges, is found on the external surface of red cells, and offers an elegant biomimetic solution to low fouling [5, 6]. However, a comprehensive PC layer is likely to inhibit the transport of polar diffusible species and target macromolecules to the sensing element of a biosensor.

2.3 *Conferred functional advantages of membranes*

Membrane and certain types of thin film technology may well in future make the difference between commercially viable and non-viable biochips. They could confer a

Table 1. Key surface properties of polymeric membranes.

Chemistry	Polar, charged, H-bonded, hydrophobic, ionizable
Mobility	Backbone, sidechain, plasticizer mobility
Topography	Roughness (molecular, cellular), irregular/regular pattern porosity, pinholes

Table 2. Benefits offered to biosensors by use of membrane technologies.

Membrane technology
• Surface modification • Aperture control • Chemical 'gate' • Sample clean up • Interferent control • *In vivo* biocompatibility
↓
Without surface modifications, biochips are vulnerable.

variety of benefits, which reduce the high level intrinsic specifications demanded of microfabricated biochips, so serving as a useful complementary technology (table 2). Surface modification allows adaptation of the base materials used for biochip production. Aperture control through pore size management, allows for reduction of analyte access to the device, and therefore, without sample dilution to enable the biochip to operate at concentration ranges where biocomponent binding would normally be saturated. At high concentrations, bioaffinity is zero order with respect to concentration, and the biosensor thereby of little use. If the membrane has surface attached pendent groups, then solute transfer through its pores will be affected by solute/wall interactions; the greater the interaction, the lower the transport. Such chemical 'gating', whilst not often used, could resolve mixtures of similar solutes and so underpin resolution by biochip arrays. Sample clean up may similarly be achieved; there are significant advantages to allowing biosensor detection reactions to be fully partitioned from the sample itself. For interferent control, generally a homogeneous or reverse osmosis type membrane is used, as here microsolutes may need to be rejected.

2.4 *Interfacing of biosensors* in vivo

In vivo biocompatibility is a special sub-field of biosensor research. A biocomponent within a biosensor has to be entirely immunologically sequestered and unavailable for contact with the body. Moreover, the biosensor components must be non-toxic, non-tetratogenic, non-carcinogenic, non-irritant, and neither degrade to release toxic agents nor generate reaction products that are toxic and lead to indirect tissue damage. In absolute terms many of these specifications are unattainable, however, the right choice of membrane materials is able to slow up adverse effects sufficiently to minimise the interfacing risk both to the patient and to the biosensor.

Blood interfacing poses special challenges. Microfabricated biosensors have the potential to reduce adverse effects, since the implant materials burden would be small, however, the intravascular compartment is still a dangerous environment. Not only is there the high risk of surface coagulation, but clot dissemination (embolism) and associated microthrombus cascades pose risks that are unacceptable for a diagnostic device. Some progress has been made through use of surface immobilized anticoagulants as shown with heparinized surfaces [7–9], but however effective the surface anti-coagulant, coagulation is still triggered if there is any platelet activating flow turbulence close to the device – a likelihood with any probe inserted through the vascular wall.

Table 3. Membrane materials used.

Membrane types	
• PVC	• Silane
• PVC–lipid	• Sulphonated-PEES
• PVC–surfactant	• Polycarbonate
• Diamond-like carbon	• Electropolymerized films
• Cellulose acetate	• Bi-layer lipid membranes
• Polyurethane	

2.5 *Membrane systems used*

Considerable versatility and ingenuity is required to translate membrane fabrication techniques at the macro-scale to the microfabrication of biosensors. Our past work has emphasized the former, and in general, solvent casting of preformed polymers has been used to coat planar and needle-shaped electrodes. Such techniques could be utilized for biochips, to lay down conventional thick films (table 3), but more attention needs to be paid to edge effects and ambient solvent evaporation conditions for microsurfaces.

More amenable to microscale deposition is *in situ* monomer electropolymerization. Whilst a conducting surface is obligatory for such a coating process, deposition can be highly controlled and solvent-related edge effects eliminated. Electropolymerized films, if conducting, can provide a further means of interrogating the biolayer if bio-layer binding to a target is associated with a charge related or conductivity behaviour modification of the film.

3. Thick membrane films at electrochemical sensors

3.1 *Microporous membranes*

Microporous membranes based on polycarbonate through which linear track micron diameter pores have been etched, are in common use for particle separation. They are an ideal non-swelling structure for partial colloid and cell separation. In the context of biosensors, the pore size (and pore density) may be independently controlled, and therefore an aperture for driving down transport of a diffusible target solute into the biosensor. In particular for oxidase based sensors:

$$\text{Substrate} + O_2 \rightarrow \text{product} + H_2O_2 \quad (1)$$

such as that for glucose and lactate, the low Michaelis constant (K_m) thereby extends to beyond the upper concentration range of the fluid to be analysed, O_2 demand is reduced and so an effective linear dynamic biosensor range may be engineered. The low permeability furthermore eliminates bulk convective flow influences such that a sample viscosity and stirring independent system results [10].

Microporous polycarbonate may be further modified with an outer coating of diamond-like carbon (an amorphous H, C alloy without a crystalline domain). A diamond-like carbon nanofilm has high haemocompatibility [11], and because it is deposited from a plasma source, exquisite control over coating thickness and therefore membrane aperture is possible.

Silicones deposited on a microporous membrane [12] also control pore aperture, but because the silicone is O_2 permeable, and impermeable to organics, a larger aperture for O_2 is afforded than for the metabolite substrates such as glucose, pyruvate or oxalate – key medically important measurement target. This allows oxidase-activated biosensors to be produced with extended linear responses, since the reaction (equation (1)) is then even less oxygen demanding.

Covering silane films variously produced from the cross-linking of di- or tri-halogen substituted silane monomers also give a better haemocompatibility than the base material. A planar microelectrode array utilizing the oxidase route for measurement, could in principle be covered with a single microporous membrane, and variously coated with modifying films of silicone or diamond-like carbon to create a family of sensors with a spectrum of sensitivities (calibration slopes) and linear limits to allow for multiple redundancy, statistical data acquisition, drift-free measurement and higher data security. The challenge is for membrane coating techniques to be carried out on a length scale that matches biochip fabrication.

3.2 *Homogenous membranes for transport control*

Cuprophan® is an established regenerated cellulosic membrane used for medical haemodialysis. It is crystalloid permeable, colloid rejecting, and non-toxic. As such it has been used in many reports in the past as a covering barrier layer for enzyme based biosensors. Its drawback is that permeability and selectivity cannot be readily altered.

PVC is at first examination an unpromising material for selective separation or controlled dialytic transport; it is organic solute impermeable. It is, however, an excellent support matrix for surfactants [13, 14]. Surfactants have the effect of separating polymer chains to create voids for solute transport, so the effect should be a general one. In figure 1, cellulose acetate supported a methyl trialcyl cationic quaternary ammonium ion surfactant (MTAC) and allowed transport of anionic pyruvate.

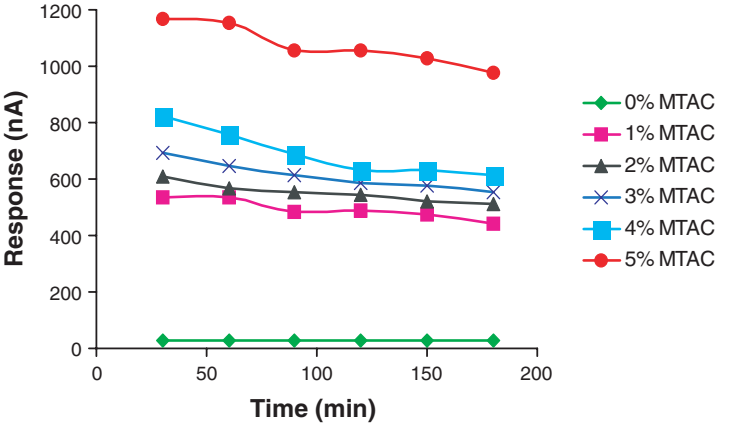

Figure 1. The cationic surfactant (MTAC) is incorporated into cellulose acetate (CA) as an outer membrane coating for pyruvate. As the surfactant content increased the effective response of the sensor also increased due to increased retention of co-factor within the proximity of the working electrode.

Importantly, the membrane-entrapped cation was able to retain cationic charged cofactors for the enzyme, so a relatively low drift resulted even in cofactor free sample.

Membrane materials have the potential to accommodate fluid microflows, and with judicial choice of the carrier surface (as with surface fouling), the affinity of mobile macromolecules can be modified and their transport behaviour controlled.

4. Non-conducting electropolymerized films

4.1 *Basic advantages*

Electropolymerization of ultrathin films on working electrode materials is a means of film coating that is used with equal facility for macro-scale and micro-scale electrodes. The basic electrode surface, however, develops a protective layer analogous to the use of such films previously for corrosion protection. The functional aim here, however, is to produce low molecular weight cut-off films notably again to select for H_2O_2, the primary product for biosensing of oxidase catalysed reactions (equation (1)). Such films may also improve haemocompatibility, extend the linear range for the analyte of interest, and indeed help better understand the interactions between sample and sensor surface.

4.2 *Polyphenolic films, their biocompatibility and selectivity*

The electro-oxidation of phenol in solution produces a half wave at $\sim$+0.65 V *versus* Ag/AgCl, and no reduction wave on reversing the voltage sweep in cyclic voltammetry (figure 2). This is confirmatory evidence of a stable, inert film on the electrode, which accumulates on multiple sweeps until a limiting insulating layer is formed which precludes monophenol oxidation. This film layer provides for an entirely different selectivity profile for the device (figure 3) which in particular is seen to be relatively accessible to H_2O_2 whilst largely eliminating transport of common blood interferents; catechol here is not a constituent in blood, but a potential end product

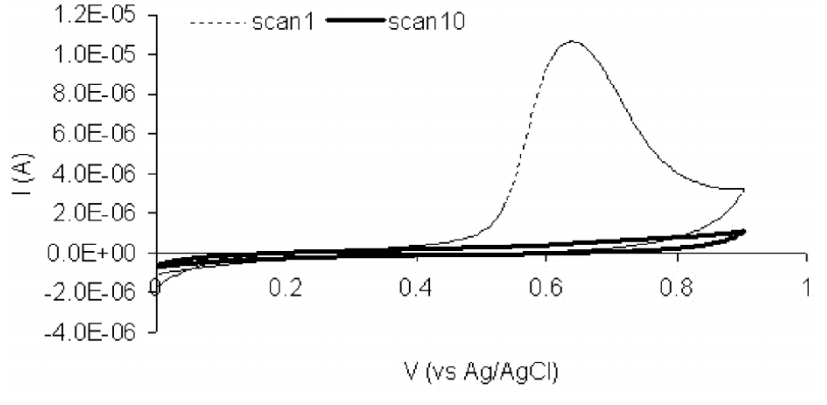

Figure 2. Electropolymerization of phenol (10 mM in PBS pH 7.4) on Pt working electrode. Scan rate 50 mV s^{-1}. Following initial oxidative wave at +0.65 V *vs.* Ag/AgCl due to electro-oxidation of monomeric phenol, polymerization occurs such that Pt becomes insulated preventing further oxidation of phenol. The process is therefore self-limiting.

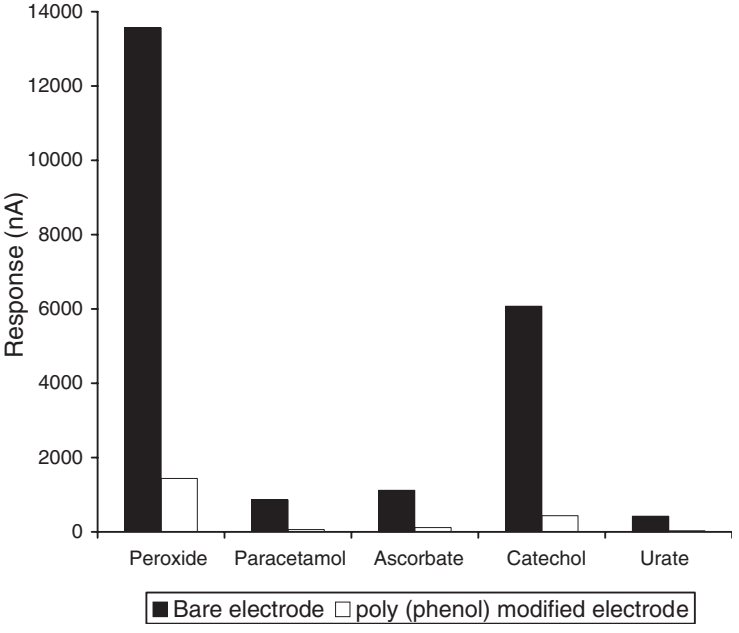

Figure 3. Effect of polyphenol modification on selectivity profile of Pt.

of a redox indicator reaction cascade usable for monitoring dehydrogenase reactions [15, 16].

The haemocompatibility of a surface is improved by polyphenol, and whilst some drift is observed, the comparison with the bare electrode is highly favourable (figure 4). The films may also have advantages not only for microfabricated structures used in blood but in protein loaded solutions as might be considered for proteomic arrays.

4.3 *Polyphenol variants*

Phenolics with more complex structures and pendent groups would be expected to give modified selectivity and biocompatibility performance, and a range of these have been tested (figure 5). Of these poly(rosolic acid) appeared to be the most suitable (figure 6). There is further possible manipulation of the interface using different conditions; polymerization is more rapid at higher potentials and the net charge requirement lower. These are free radical propagated polymerizations following the initial phenol oxidation, so forming efficiencies might be expected to be different. Higher solution pH gives more porous films, and selectivity is a cumulative effect depending upon deposition times, so individual films may be tailored or used in systematically varied biochip arrays.

4.4 *Polyphenols with surfactant entrapment*

Polyphenols provide for entrapment of 'bystander' solutes in solution provided these are of sufficiently high molecular weight. Surfactants are of interest, since not only

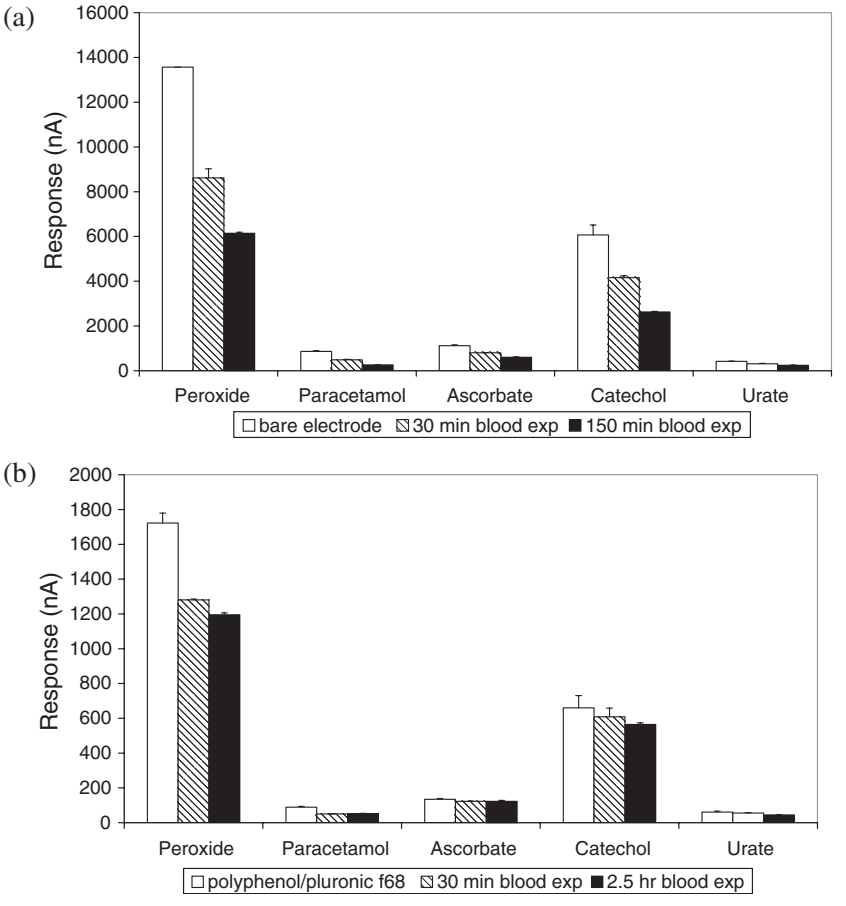

Figure 4. (a) Susceptibility of bare Pt working electrode to whole blood exposure. (b) Stabilization of Pt working electrode to whole blood exposure through polyphenol modification.

are they sufficiently large to be physically entrapped in the films, but their solubilizing effects and variable charge properties (table 4) would help confer a modified function on the films, with possibly better haemocompatibility; figure 7 indicates that fouling in blood may be reduced over time. In all instances with film coats, the level of stability in blood is excellent compared with a bare electrode (figure 8). This data strongly indicates that the base Pt (and other) electrode materials are not sufficiently reliable for use in biofluids however sophisticated the biochip array maybe unless some specific means of guarding against fouling has been used.

5. Conducting polymer films

5.1 *Utility for biosensors and basic constructs*

Planar conducting films whilst potentially usable as a membrane barrier, or a biocompatibility inducing interface, can also operate as reporters for bioaffinity reactions, and

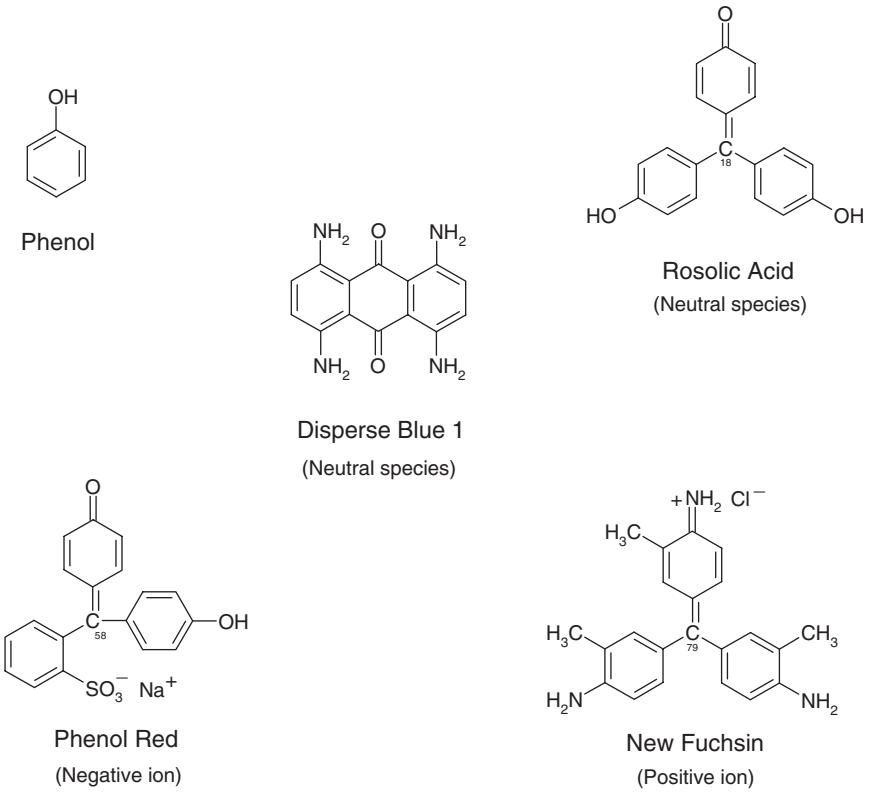

Figure 5. Selection of phenolic monomers used during formation of electropolymerized coatings on Pt working electrodes.

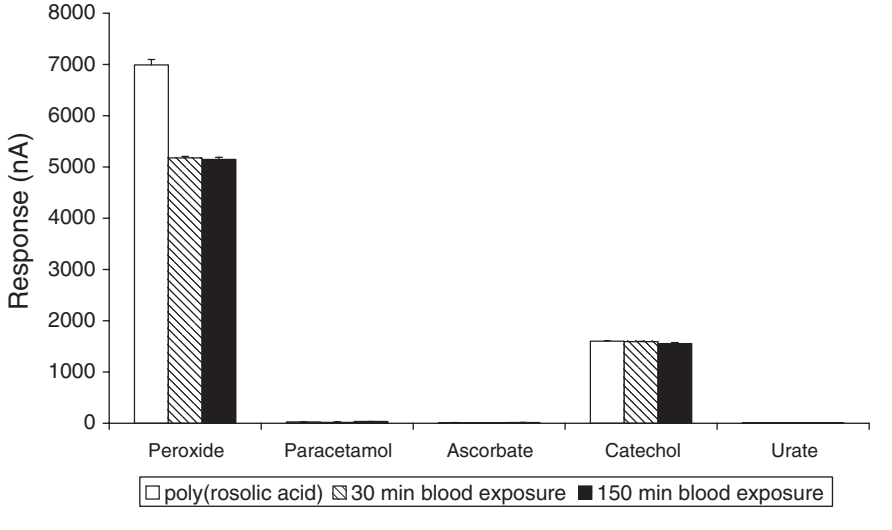

Figure 6. Selectivity of Pt modified with poly(rosolic acid) coating following exposure to whole blood.

Table 4. Surfactants used for entrapment in polyphenols.

Surfactant	Polarity	Formula weight ($g\,mol^{-1}$)	Critical micelle concentration (cmc)
Pluronic F68	Pluronic F68	8400	100
Adogen 464 (methyltrialkyl (C8–C10) ammonium chloride)	Cationic	368–452	n/a
Taurocholic acid	Anionic	537.7	6.7

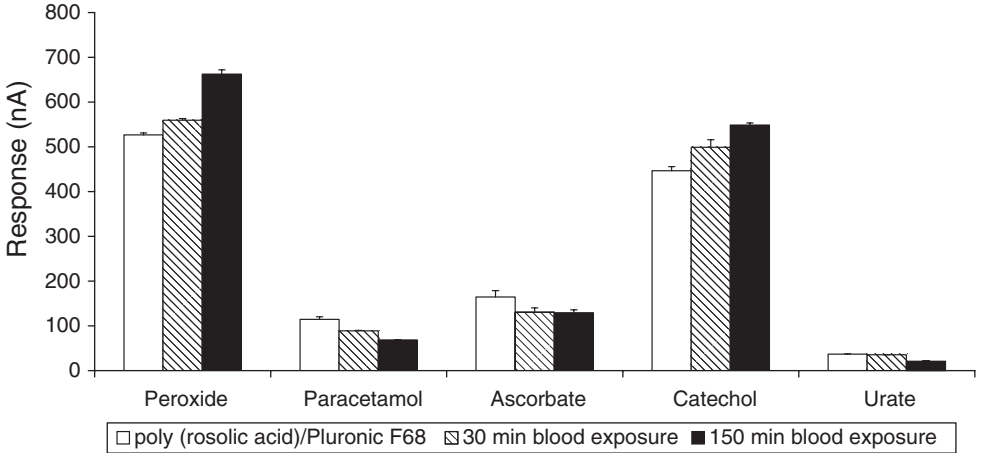

Figure 7. Effects of incorporating surfactant within poly(rosolic acid) film on stability of Pt electrode following exposure to whole blood.

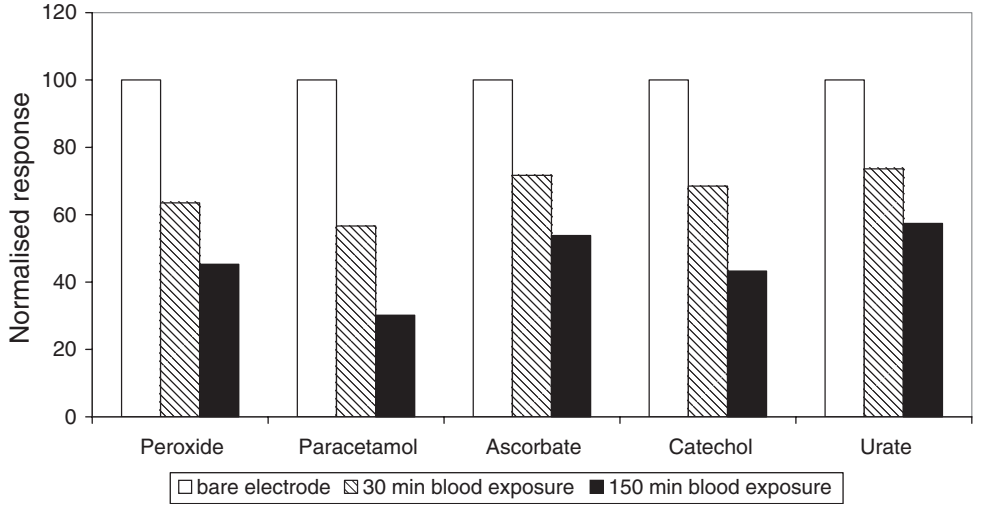

Figure 8. Reduction in sensitivity of bare Pt following exposure to whole blood, shown as normalized response.

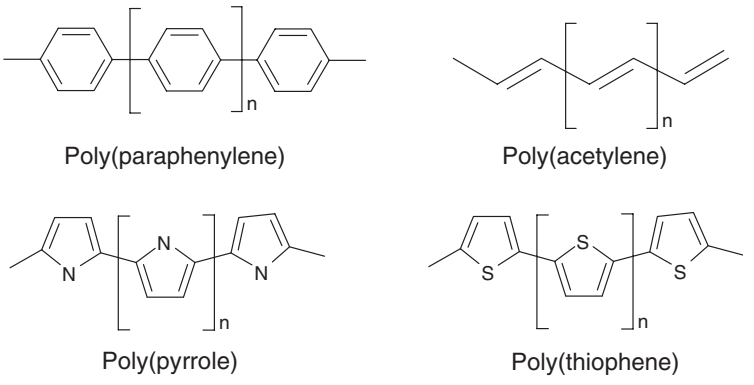

Figure 9. Species used for the formation of conducting polymer systems.

moreover can be formed over microelectrodes with the ease of non-conducting phenolics [17]. A range of organics have been used for forming conducting films (figure 9), but polypyrrole has been especially advantageous.

Conducting polymers can be switched between conducting and insulating states. Film conductivity correlates with the prevalence of mobile cation radicals (polarons/bipolarons) available on the polymer backbone [18]. Polaronic conductivity is due to delocalized positive charge spread over four pyrrole units, whereas electronic conductivity involves the conduction band of the polymer. The films generally used in aqueous solution demand relatively low potentials for redox switching and change to the state of conductivity.

Film deposition is initiated by the oxidation of a monomer to produce a radical cation, which then reacts with other monomers or monomer radicals to go to a dimer stage. Oligomer formation then moves on to nucleation and polymer elongation. Importantly the charged polymer incorporates solution anions, and if these anions are bioreceptors, then a biosensor results. The bioreceptor may be co-entrapped in the films without formal charge based incorporation, provided a simple anion is present in solution to facilitate polymerization. Inorganic anions as well as anionic oligostructures such as sodium dodecyl sulphate (SDS) and toluene sulphonate can be entrapped as stabilizing counter ions.

5.2 *Conducting polymer electropolymerization*

A planar two electrode arrangement (figure 10) comprising interdigitated Au electrodes if used as a polarizable electrode can allow surface deposition of polypyrrole. Once nucleation has occurred, film growth can be followed during cyclic voltammetry (figure 11). The counterion incorporated affects the voltammetry signatures of formed films, seen especially for reduction peaks (figure 12). The avidin-incorporated film when used as a receptor for D-biotin, however, shows little further effect on the cyclic voltammogram. This would seem to indicate that voltammetry is not an appropriate means of detecting receptor changes in polypyrrole, and some alternative is required.

Interdigitated structures (figure 13) can be bridged by means of polypyrrole, and bridging can then be used to measure film conductivity with any given counterion.

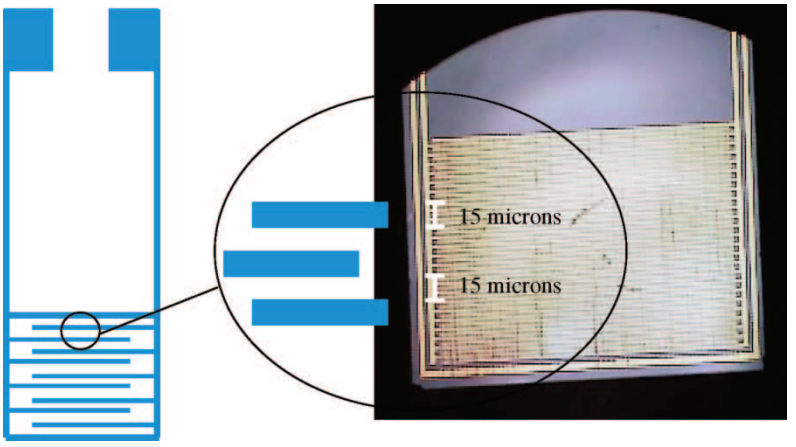

Figure 10. Electrode arrangement for planar film impedance spectroscopy. The image shows optical microscope image of the electrode on the right and a schematic on the left indicating the 15 μm gap between electrode fingers.

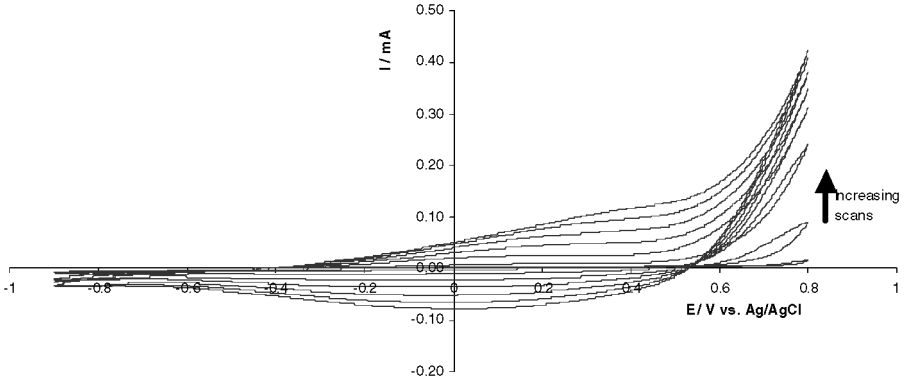

Figure 11. Formation of polypyrrole as monitored by cyclic voltammetry. There is a continued increase in the magnitude of the oxidative wave with subsequent potential scans.

To do this, a low ionic strength solution is needed to maximize uptake of a receptor molecule and to control the extent of bridging achieved between electrodes. A relatively high polypyrrole concentration is also needed to avoid inhibition of film growth. It is important to recognize that film structure may vary with the counter ion. SDS leads to confluent growth (figure 14) and avidin is associated with discoid, multipoint growth; such variation may have an effect on analyte access to the film, affecting available surface area for such binding and the degree to which non-specific surface binding of proteins and cells occurs at the sample interface.

5.3 *Impedance spectroscopy at planar polypyrrole films*

Once formed on a surface the polypyrrole film can be switched from an insulating to conducting state, based on the impressed polarizing voltage. However, a particular

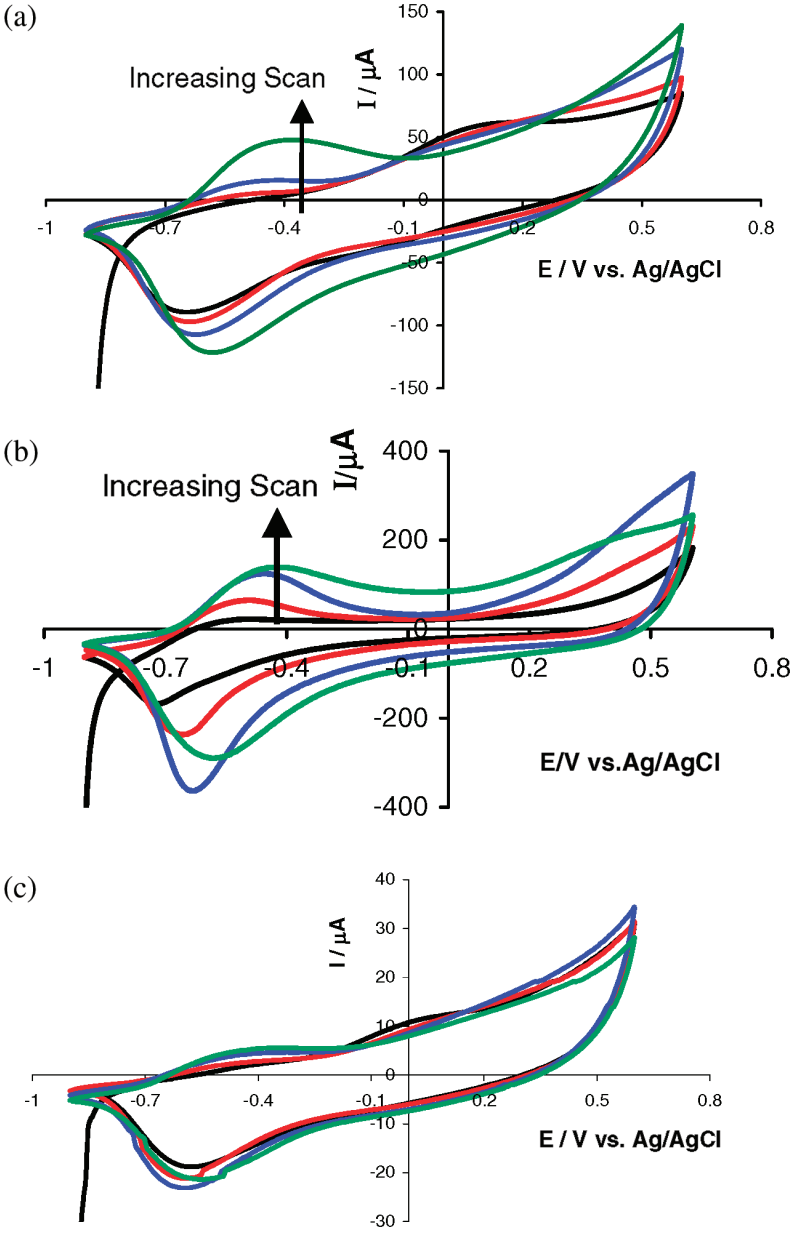

Figure 12. Effect of incorporated counterion on the reduction peak signature of poly(pyrrole). (a) Poly(pyrrole) film. (b) Poly(pyrrole) film containing SDS. (c) Poly(pyrrole) film containing avidin. Arrows are in direction of CV sequences.

redox state can also be sustained, determined by some intermediate polarizing voltage. The set redox state can then be followed by two-electrode electrochemical impedance spectroscopy (EIS).

Two electrode EIS can be achieved using a 20 mV RMS sinusoidal potential, and an impedimetric spectrum taken between an extensive frequency range, viz. 5 Hz

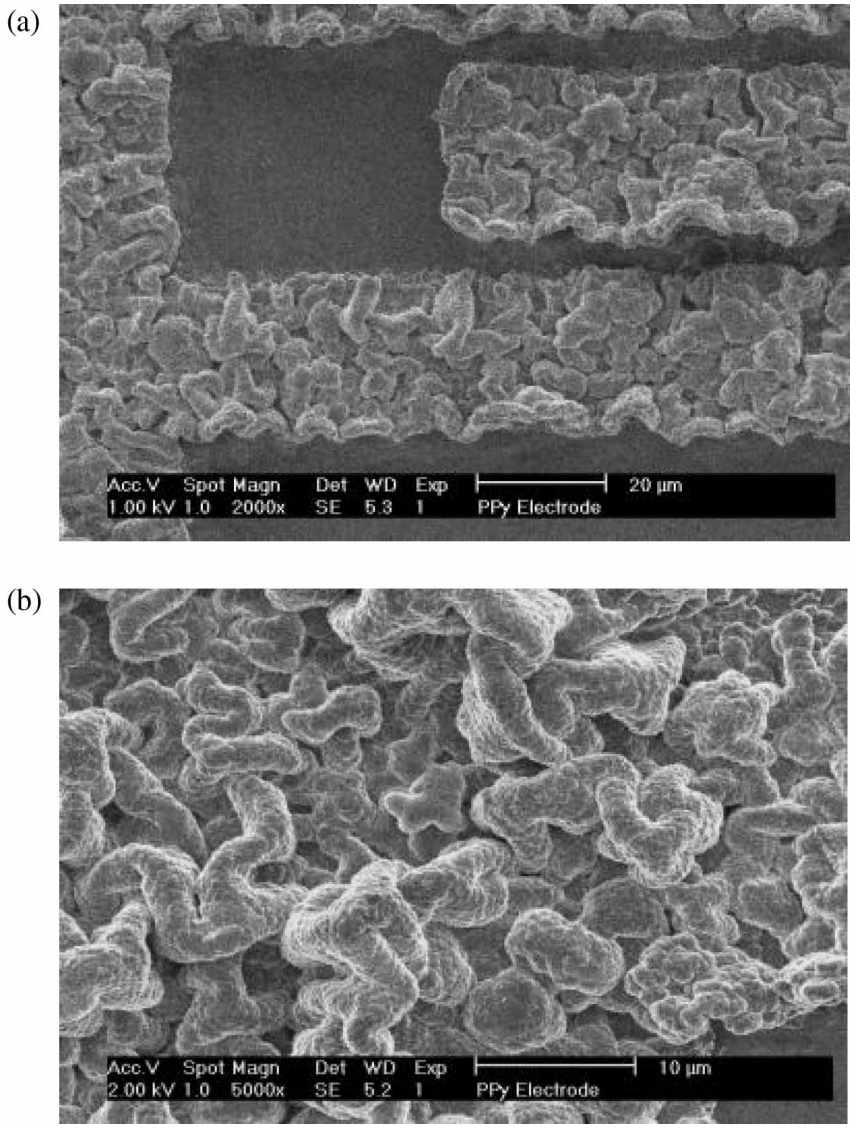

Figure 13. Images of 15 µm gap gold IDE that has been surface modified with poly(pyrrole). (a) SEM image showing coverage of IDE structure (see figure 16) with poly(pyrrole). (b) As (a) at increased magnification showing detail of poly(pyrrole) surface morphology.

to 13 MHz. Independent measures of polaronic and electronic conduction can be obtained, since they take place on quite different voltage oscillatory time scales.

A Bode plot is a useful graphical representation of impedance data, combining capacitive current measurement (out of phase with sinusoidal voltage) with impedance measurement (in phase with sinusoidal voltage). Impedance (z) defines the relationship between applied potential and current, and more formally is a vector quantity composed of a real (in phase Z') and an imaginary (out of phase Z'') part related by $Z = Z' + jZ''$ (where j is the complex number, $\sqrt{-1}$) and the modulus

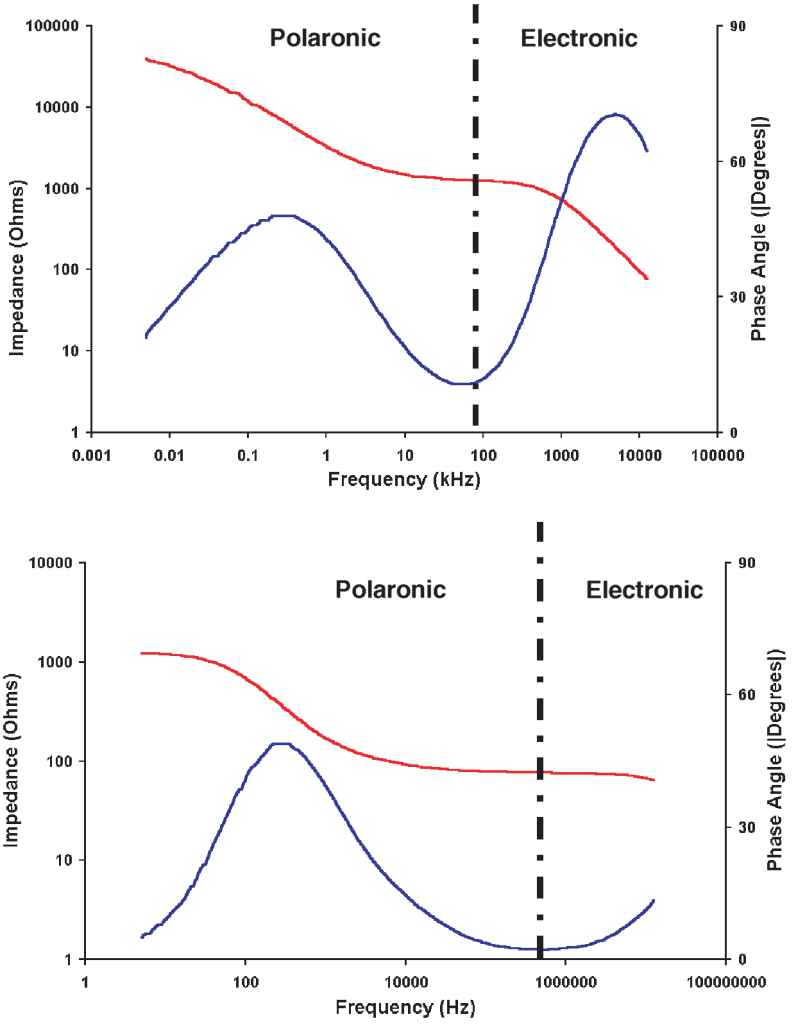

Figure 14. Two electrode impedance spectra at IDEs.

$|Z| = (Z'^2 + Z''^2)^{0.5}$. Physical interpretation of the data is problematic, but the observed data is commonly modelled using derived equivalent circuits comprising arrangements of resistors, inductors and capacitors. In practical terms, an electroinactive product or outcome of a bioaffinity reaction can be registered and a two-electrode arrangement is usable, provided film redox state is remains stable. Real films show distinct separate zones respectively of electronic and polaronic conduction (figure 14). In ionic solutions, such as with phosphate buffer, polaronic conduction is augmented because the presence of the mobile anions in a film facilitates charged-linked electron transfer.

5.4 *Impedimetric measurements of LH and biotin*

For a model system incorporating antibody to lutenizing hormone (LH) a polaronic phase is identifiable (figure 15), but more importantly, there is a capacitance reduction

and an impedance increase after binding to LH. Notably this is seen only when a redox cycle is imposed post-binding. This provides indication not only of how an antibody can be entrapped within polypyrrole yet remain active and accessible to a peptide such as LH, but how in the absence of any apparent voltammetric changes, the impedimetric signature is altered to thereby achieve reagentless, binding recognition. The inherent principle should be translatable to other affinity pairs. Thus for avidin entrapped in polypyrrole, responses are seen for biotin and biotin analogues that are significantly different from an entrapped urease control with regard to phase angle (figure 16a). The biotin derivatives used are amidocaproate succinimide ester

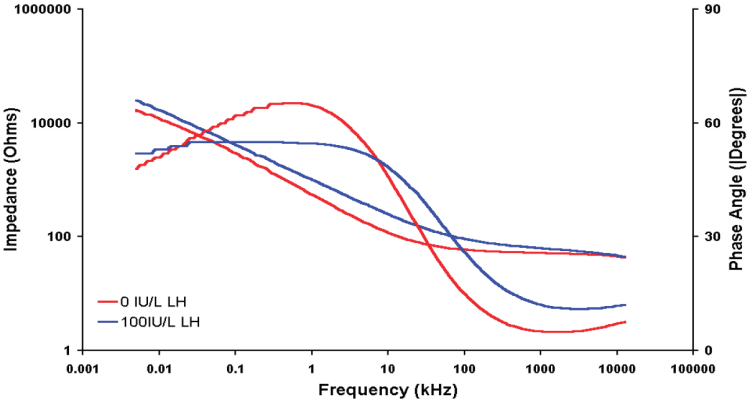

Figure 15. Reagentless binding with LH–upper capacitance peak, and lower impedance curve trace the zero LH response. LH concentration 100 IU/L.

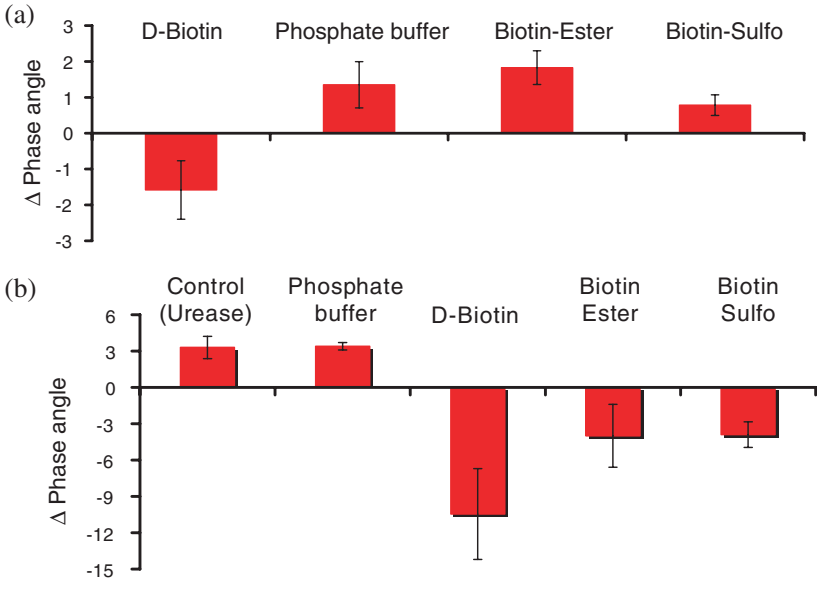

Figure 16. Effect of base IDE condition on polypyrrole film formation. (a) Unused electrode, (b) recycled electrode.

(biotin ester) and biotin amidocaproate 3-sulpho ester (biotin sulpho). There is firstly an increase in phase angle seen on exposure to phosphate buffer, and this is a background effect that would need to be taken into account even if practical measurements are carried out, but the effect of biotin binding is clear-cut.

A key feature of all observed binding induced phase angle changes is the need for one preliminary redox cycling step to unmask the effect on capacitive behaviour (phase angle). Possibly such cycling allows for realignment of polymer chains around the newly formed complex, in turn changing polymer conformation, and therefore ring alignment and polaronic conduction.

The importance of the original gold-polypyrrole surface in conditioning the response is illustrated (figure 16b) in the lack of significant biotin response where an electrode had been reused following formic acid cleaning to remove previous films. The subtlety of this effect is underlined by the finding of basic Bode plot profiles for recycled electrodes that are identical to unused electrodes. Thus, either the gold electrode interface is directly important for conditioning cross-IDE impedance, or the gold surface affects the superimposed film structure.

The avidin biotin complex is a useful model to study, but the high binding affinity of avidin ($K_D = 10^{-15}$ L/M) does not readily allow concentration dependent effects to be followed. These, however, can be seen for an LH–antibody combination, but it is also notable that with the polyclonal antibody preparation used, notwithstanding a high LH affinity, there was little response in contrast to a monoclonal antibody. Possible reasons for this include blocking contaminants in the polyclonal preparation, molecular heterogeneity distorting polymer conformation changes following binding, antibody aggregates reducing microenvironmental effects within the bulk of the film structure.

The monoclonal–LH system demonstrated no significant response in phosphate buffer, but response to LH was attenuated by pre-incubation of the LH with bovine serum albumin ($3\,g\,L^{-1}$), tested up to 800 IU/L LH. The albumin possibly blocked binding, or there may have been bulk solution associated effects with LH that prevent antibody interaction. Whatever the reason, such complex macromoleculer interactions highlight a further challenge to measurements in biological samples. This is in marked contrast to the use of impedimetric measurements at conducting polymers for gas phase affinity sensing, as developed for artificial nose technology [19] where interferences are minimal.

5.5 *Cole–Cole plots for DNA hybridization*

A DNA hybridization experiment is commonly conducted in controlled buffer solution, and so is more amenable to interference free impedimetric analysis. Cole–Cole plots offer an alternative characterization regimen to the Bode plot. Here, real impedance is plotted against imaginary impedance over a wide AC frequency range. Analysis of these plots can provide quantitative information about the interfacial region between the electrode and the electrolyte, between surface adsorbed layers on the electrode and between layers within the electrode structure. For example, a vertical straight line in a plot indicates a capacitive or insulating system. Such a curve can be obtained from a metal layer coated with protective film. The film covers the electrode and thus impedes the movement of charge out from the electrode and so charge accumulates within the metal layer causing this to act as a capacitor. If the film begins to corrode

at a uniform rate then a there begins to be a transfer of charge from the electrode to the surrounding electrolyte. The Cole–Cole plot obtained for this system would show a semi-circle that intercepts the *x*-axis (real impedance axis) at two points. The point nearest the origin is the high frequency intercept and is a measure of the solution resistance. The point furthest from the origin (the low frequency intercept) is the sum of the solution resistance and the polarisation resistance; therefore the polarisation resistance is simply the diameter of the semi-circle. Analysis of the arc can also produce quantitative estimates of conductivity, Faradic reaction rates, relaxation times and interfacial capacitance.

When DNA modified sensor surfaces are produced by adsorbing oligonucleotide sequences onto gold IDEs as single or prehybridized (double stranded) DNA, quite different Cole–Cole plots are obtained (figure 17). This dramatic difference is seen after pyrrole monomer is cycled ($\times 5$) between -0.9 and $+0.9$ V against Ag/AgCl reference electrode with a Pt foil counter electrode. This provides a possible means of DNA sensing. The mechanism for the difference is obscure, but polypyrrole possibly was able to intercalate within the double stranded groove, thus leading to the altered signature.

The impedance measurement of a bare interdigitated electrode results in a near vertical line indicating purely capacitive behaviour; which is to be expected since the individual digits of the electrode do not provide a route to a complete circuit between adjacent digits and so charge accumulates within the electrode. The adsorption of single-stranded DNA to the electrode surface followed by cycling in pyrrole monomer leads to a similar Cole–Cole plot, indicating that once again no complete circuit is formed. Minor differences observed may be due to polypyrrole directly modifying the electrode surface. The adsorption of double-stranded DNA and cycling in pyrrole suggests the presence of a charge transfer process indicating that either the double-stranded DNA, or the combination of the double-stranded DNA with the pyrrole, creates a closed circuit allowing charge transfer in the plane of the electrode.

Certainly there is indication that the morphology of the films formed at single *versus* double stranded DNA coated gold electrodes is quite different at 5 cycles (figure 18).

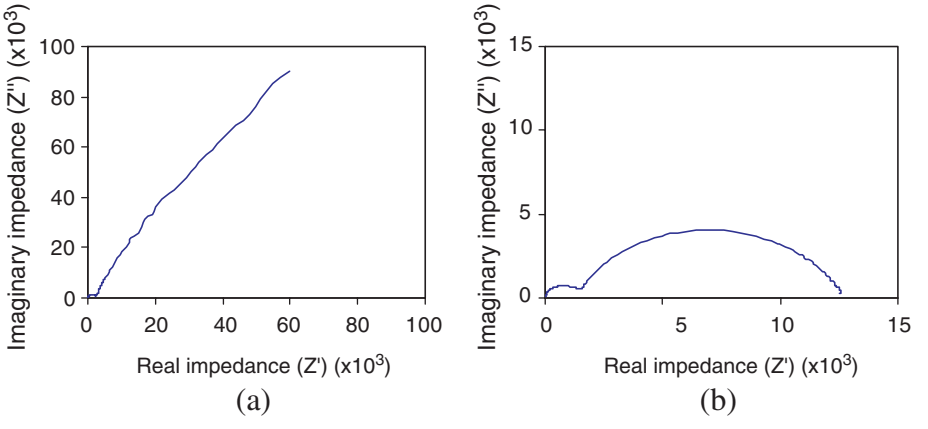

Figure 17. (a) Plot of single-stranded DNA absorbed at IDE and following cyclic voltammetry in 0.5 pyrrole in phosphate buffer. (b) Plot of double-stranded DNA following same protocol.

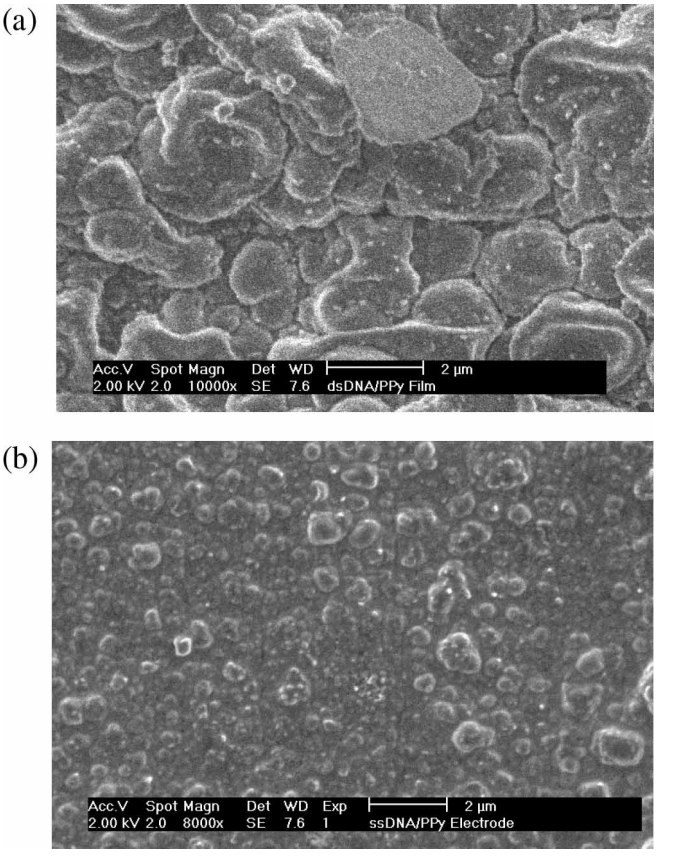

Figure 18. SEM highlights differences in film morphology with, (a) double-stranded DNA + pyrrole and (b) single-stranded DNA + pyrrole; both following 5 redox cycles in phosphate buffer.

How such surface morphology is linked to a remote subjacent layer of single *versus* double-stranded DNA, and what effects of phosphate ion adsorption there may have been remains to be worked out.

6. Microflows as surrogate, renewable barrier films

6.1 *Needle biosensors and* in vivo *monitoring*

Notwithstanding the structural elegance and geometrical precision of MEMs based sensors for *in vitro* use, *in vivo* insertion even for percutaneous blood sampling and intravenous lines still relies upon needled technology. The fundamental point is that the cylindrical geometry, miniaturization and high mechanical specification of needles satisfy the dominant issues for healthcare use and take precedence over structural and length scale elegance of MEMs devices. In the case of Si fabricated devices, there is a further concern over long term implantation, in that dissolution of Si and local elemental release may be of significance, an issue that needs quantitative consideration if say porous Si is to be used for *in vivo* device construction.

The needle design has been consistently used for implantable enzyme-based biosensors. Inevitably the greatest attention has been paid to glucose sensing in view of the healthcare importance of diabetes. One classic construction route for this has used two functional layers aside from the chemically cross-linked enzyme layer of glucose oxidase [10]. The first layer is a selective low molecular weight cut off barrier based on a sulphonated polyether ether sulphone–polyethersulphone (SPEES–PES). This robust ionomeric barrier mostly excludes ascorbate, urate and acetaminophen (Tylenol®) as major electrochemically active interferents on the combined basis of size and charge. The degree of sulphonation is important, and may explain why a high selectivity has not been seen by some [20]. The outer layer, covering the antigenic enzyme layer must interface with the biofluid, and is a multilayer porous polyurethane serving to reduce glucose transport to the enzyme layer, retain O_2 transport (equation (1)) whilst providing mechanical integrity and high resistance to the degradative action of free radicals initiated by neutrophil attack. The laminate formulation used by us is a combination of five pre-polymer polyurethane layers and a single carbonate polyurethane (Corethane®) outermost layer known for its tissue compatibility and low degradation rates.

6.2 *Open mircoflow for* in vivo *monitoring*

Needle glucose electrodes used in tissue for short-term (~24 h) monitoring are acceptable for diabetic home use, in principle. In practice though, percutaneous, temporary insertion for such minimally invasive monitoring is difficult to achieve. However stable such devices are *in vitro*, including in blood, the tissue response to the implant demands firstly a stabilization period of some hours, and then *in vivo* calibration, as tissue: blood glucose values neither at steady state nor under dynamic conditions show a clinically acceptable match for nearly all current devices. The reasons for this are complex, and reflect transcapillary transport lag time, the limit of the microcirculation to supply and remove glucose, the nature of the inflammatory exudative tissue response and the distance between the capillary bed and the implanted sensing surface. The last is compounded by the barrier function of the interstitial tissue 'mesh'.

Open microflow (figure 19) allows for delivery to the tissue implant site of a film of hydration fluid delivered over the sensing surface of the device and then into the tissue itself. Because subcutaneous tissue mostly operates at a negative hydrostatic pressure, fluid transport does not necessarily require physical pumping and at a net outflow diameter of 0.2 mm, 1–2 μL of buffer enters the tissue per minute. The amounts are therefore extremely low, and well within the range of volume exchanges that occur at the capillary bed under physiological conditions, as driven by net positive and negative transcapillary pressures in the Starling mechanism.

The externally reduced fluid flow creates a mobile film over the sensing surface that helps to reduce colloid/cell access to the sensor and reduces fouling. Equally important, the juxtaposed tissue is hydrated, and such hydration of connective tissue reduces the diffusional barrier presented to microsolutes. Hydraulic permeability of oedema tissue, for example, is known to be increased several orders of magnitude in comparison with normal connective tissue.

The practical consequence of Open Microflow is that sensor 'run in' time is reduced from a typical 3 h to 30 min. Also the tissue : blood mismatch is reduced as is the commonly observed temporal lag (up to 12 min) for tissue glucose changes.

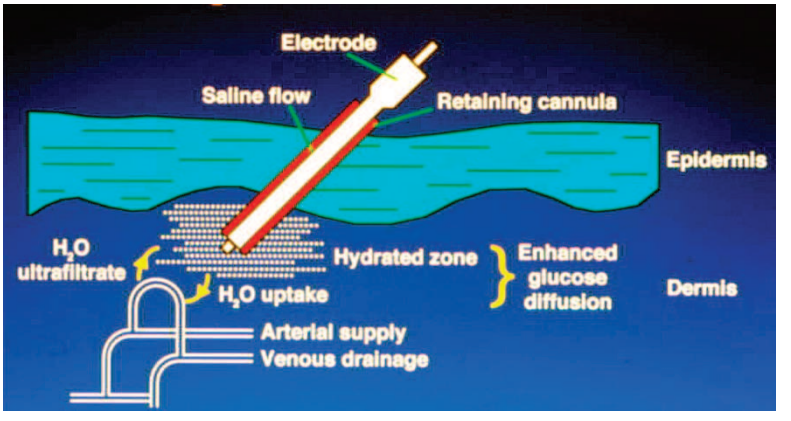

Figure 19. Percutaneously implanted needle enzyme electrode showing hydration zone at needle tip following pumpless flow of fluid into the dermis.

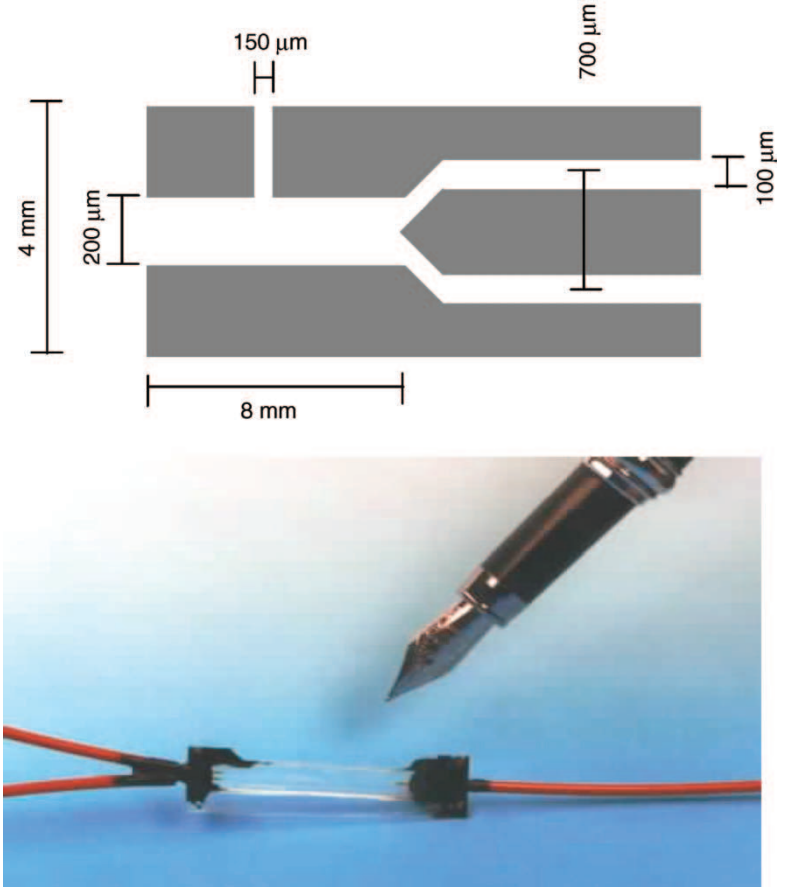

Figure 20. Bifurcated flow cell schematic (top) and (illustrated) fluidic connections for non-mixing of parallel microflow (bottom).

These advantages are most in evidence in the animal model where tissue-related monitoring error appears all but eliminated.

Translation into humans shows promise, however microfluidic design changes are a likely requirement, given the interspecies differences in connective tissue composition and capillary bed behaviour.

6.3 *Capillary flow cells for parallel microflow* in vitro

Fluid flow in miniaturized flow cells below a set threshold value that provide Reynold's numbers of <2000 permit non-turbulent fluid flow. Furthermore, parallel aqueous streams can be accommodated without interfacial mixing. The Reynolds number is proportional to {(inertial force)/(viscous force)} and is used in momentum, heat, and mass transfer to account for dynamic similarity. The equation, expressed thus, is:

$$\mathrm{Re} = \frac{DV\rho}{\mu} \tag{2}$$

where Re = Reynolds number, D = characteristic length, V = velocity, μ = viscosity, ρ = density and so there is a degree of flexibility in the flow cell construction arrangement possible. Figure 20 shows a flow cell made out of polymethylmethacrylate (PMMA) where the bifurcation is used to converge fluid streams in a 200 μm id flow channel.

During use, mixing is avoided, as illustrated for a dye loaded and clear aqueous stream (figure 21) in parallel at a flow rate of 100 μL min^{-1}. The value of this flow

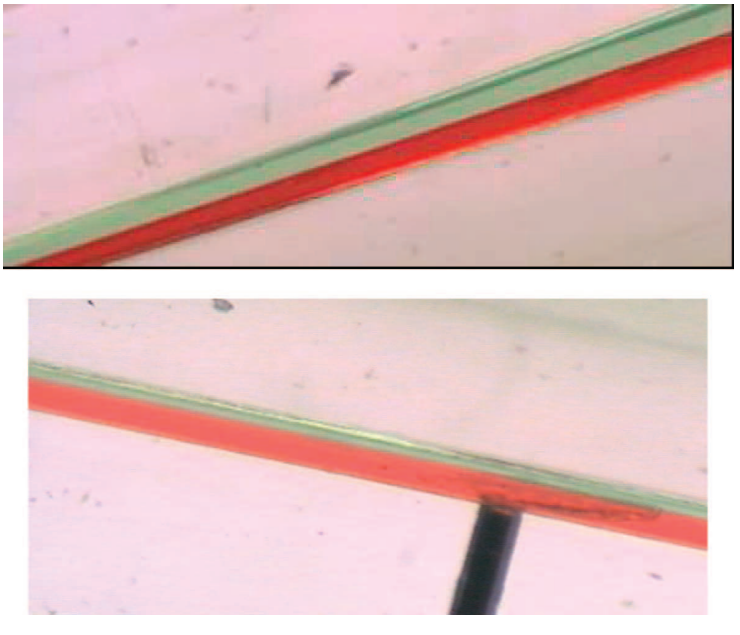

Figure 21. Dye loaded aqueous stream showing absence of turbulent mixing. Lower illustration shows *in situ* Pt electrode.

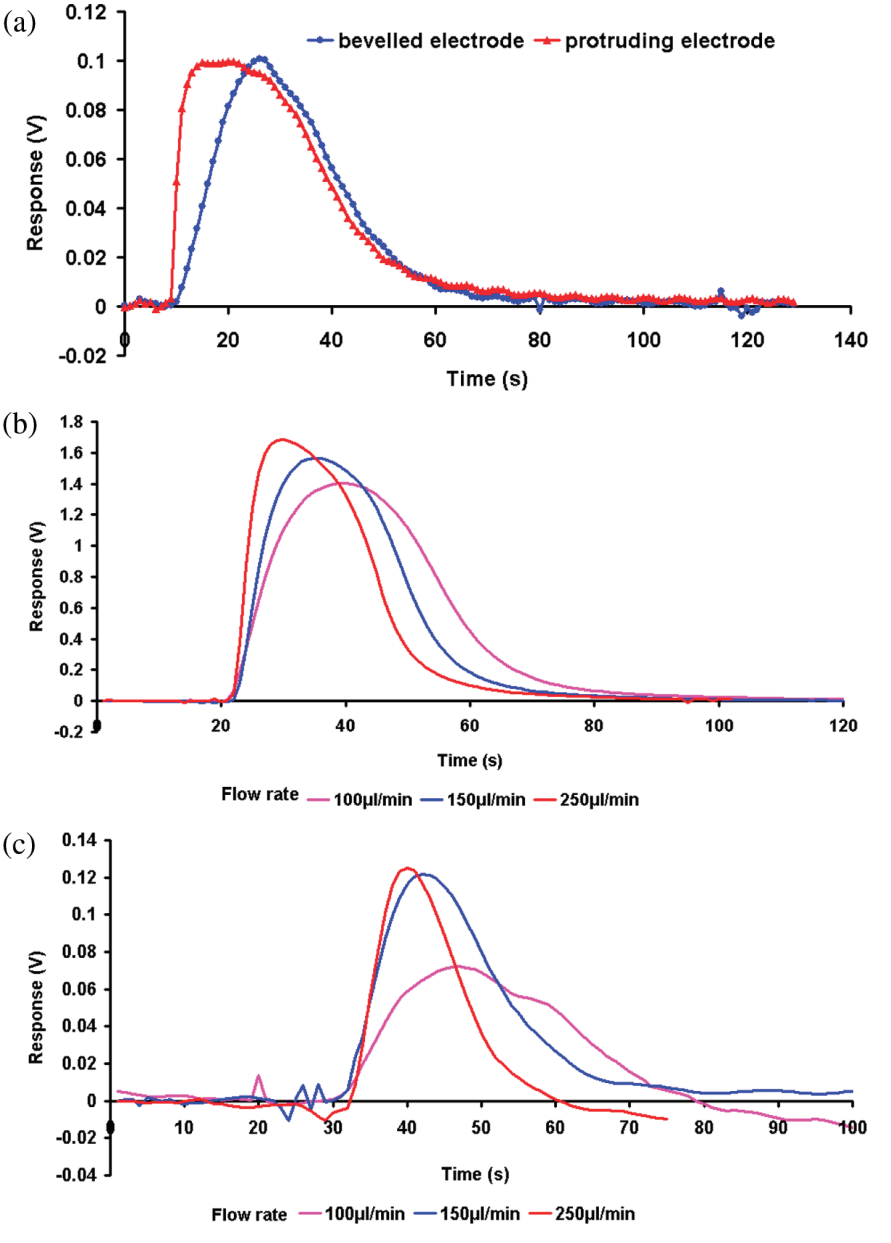

Figure 22. (a) Electrode location and flow stream relationships, (b) direct and (c) indirect as factors in sensor response. *V* represents the arbitrary readings at a current follower.

phenomenon is that (i) there is controlled laminar flow over any electrode located in the wall of the flow channel, so convective transport and therefore response of an electroactive species can be correctly modelled (ii) a protective fluid film can be used over the intramural electrode to compartmentalize the electrochemical (or chemical) detection sequence from a potentially contaminating sample stream. The protective effect primarily applies to microsolute monitoring, where diffusion coefficients are at

least one order of magnitude greater than for surface-active proteins. And moreover, cellular transport across the two streams can be virtually eliminated.

Even with a protruding electrode, it may be possible to have a viable monitoring set up, the protruding device allowing for a high exposed microsurface area and therefore higher currents (figure 22a). Flow dependence of response is inevitable at uncoated electrodes, however, an acceptable microsolute transfer and 'yield' across the parallel flows is clearly achievable (figure 22b and c).

Sample flow management in tandem with microstructure devices would be a powerful means of obtaining reliable, continuous measurements of contaminated samples. However, there will be a particular requirement in future for equally reliable micropumps and flow channel connectors.

7. Conclusion

Though biochip-based biosensors operate on a small length scale, and there is an opportunity of greater measurement reliability using multiple arrays, the need remains for reliable and stable interfacing. Relevant research in the areas of materials, membranes, fluidics and films is already available to help adapt and 'refashion' biochip surfaces for practical use. A combined effort at this stage is more likely to help deliver viable products for the future, especially in healthcare. Admittedly the advantages may only be of overwhelming importance if measurement is required on a continuous basis, or if unmodified (e.g. undiluted, non-deproteinized) samples are to be assayed. However, the over the counter medical diagnostic market is a prime example where unmodified samples will be measured, and which is likely to benefit also from biochip configurations of biosensors as truly reliable and therefore 'smart' systems, provided stability in the sample can be guaranteed.

Acknowledgements

The authors would like to thank EPSRC-RSC, JDFI, BDA and the EU for funding of the ongoing studies presented in this review.

References

[1] J.E. Pearson, A. Gill, P. Vadgama. *Ann. Clin. Bioch.*, **37**, 119 (2000).
[2] A. Pizzoferrato, C.R. Arciola, E. Cenni, G. Ciapetti, D. Granchi, L. Savarino, S. Stea. *Encyclopedic Handbook of Biomaterials and Bioengineering, Part A: Materials*, **1**, 329, Marcel Dekker, New York (1995).
[3] A. Pizzoferrato, G. Ciapetti, S. Stea, E. Cenni, C.R. Arciola, D. Granchi, L. Savarino. *Clin. Mater.*, **15**, 173 (1994).
[4] T.J. Ohara, R. Rajagopalan, A. Heller. *Anal. Chem.*, **66**, 2451 (1994).
[5] E.F. Murphy, J.R. Lu, J. Brewer, J. Russell. *Macromolecules*, **33**, 4545 (2000).
[6] E.F. Murphy, J.R. Lu, J. Brewer, J. Russell, J. Penfold. *Langmuir*, **15**, 1313 (1999).
[7] J. Black. *Biological Performance of Materials*, Chapter 9.3, Approaches of Thromboresistant Materials Development, Marcel Dekker, New York (1999).
[8] P.W. Heyman, C.S. Cho, J.C. McRea, D.B. Olsen, S.W. Kim. *J. Biomed. Mater. Res.*, **19**, 419 (1985).
[9] K.D. Park, W.G. Kim, H. Jacobs, T. Okano, S.W. Kim. *J. Biomed. Mater. Res.*, **26**, 739 (1992).

[10] S. Mutlu, M. Mutlu, P. Vadgama, E. Piskin. Sandwich-type amperometric enzyme electrodes for determination of glucose. In *Diagnostic Biosensor Polymers*, A.M. Usmani, N. Akmal (Eds), pp. 71–83, American Chemical Society Symposium Series, Washington D.C., USA (1994).
[11] S.P.J. Higson, P. Vadgama. *Anal. Chim. Acta*, **271**, 125 (1993).
[12] S. Gamburzev, P. Atanasov, E. Wilkins. *Sensor Actuat. B – Chem.*, **30**, 179 (1996).
[13] S. Reddy, P. Vadgama. *Anal. Chim. Acta*, **350**, 67 (1997).
[14] S. Reddy, P. Vadgama. *Anal. Chim. Acta*, **350**, 77 (1997).
[15] P.H. Treloar, I.M. Christie, J.W. Kane, P. Crump, A.T. Nkohkwo, P. Vadgama. *Electroanal.*, **7**, 216 (1995).
[16] S.Y. Tham, J.E. Pearson, J.W. Kane, P.H. Treloar, P. Vadgama. *Sensor Actuat.*, **50**, 204 (1998).
[17] K. Warriner, S. Higson, D. Ashworth, I. Christie, P. Vadgama. *Mater. Sci. Eng.*, **C5**, 81 (1997).
[18] G. Appel, O. Bohme, R. Mikalo, D. Schmeisser. *Chem. Phys. Lett.*, **313**, 411 (1999).
[19] P.N. Bartlett, J.M. Elliott, J.W. Gardner. *Food Technol.*, **51**, 44 (1997).
[20] Y. Benmakroha, I. Christie, M. Desai, P. Vadgama. *Analyst*, **121**, 521 (1996).